SURFACE ROUGHNESS OF ION-SPUTTERED MICROMOLD

M. Y. Ali[1*], N. K. A. Bryan[1], W. N. P. Hung[1], M. Alauddin[2], and S. Yuan[1]

[1] Precision Engineering and Nanotechnology Center
School of Mechanical and Production Engineering
Nanyang Technological University, Singapore

[2] Department of Mechanical Engineering
Bangladesh Institute of Technology, Dhaka

Abstract This paper discusses the development of mathematical models for the calculation of surface roughness of focused ion beam (FIB) sputtered microfeatures. The effective beam shape was characterized first and then the beam function was developed. Material function was developed from the inherent material properties. These two functions were then combined mathematically to develop the surface roughness models. The models were verified by sputtering single crystal silicon using 50 keV Ga ion FIB. The models were applied to fabricate microcavities which were successfully used for the replication of three dimensional (3D) polymer microcomponents.

Keywords: FIB, LIGA, Sputtering, Micromolding.

INTRODUCTION

Challenges were identified when producing 3D microcomponents with submicrometer accuracy and nanometric leveled surface finish at a reasonable cost. Such demand was needed for technical and economical realization of microsized components and systems such as microlens, optical guide, optical fiber, microgear, MEMS, MOEMS, etc. A promising technique to mass-produce the 3D microcomponents was to fabricate microcavities for subsequent replication process [Ali et al., 2000; Vasile et al., 1999]. Although the LIGA (Lithography, Electroplating and Molding) process could be used to fabricate microcavity, it was complex and required high investment and production cost [Ehrfeld and Lehr, 1995; Ruprecht et al., 1996; Weber et al. 1996]. Deep reactive ion etching and microlithography using SU-8 photoresist was a simpler and cheaper process by compromising the product's geometrical integrity and surface quality [Lorenz et al., 1997].

FIB sputtering was a promising alternative for the successful fabrication of 3D microcavities with submicrometer accuracy, and few nanometers of average surface roughness [Casey et al., 1994]. Hence, modeling of sputtered microsurfaces was sought and this paper presents analytical models that successfully predict the surface roughness of FIB sputtered microcavity on single crystal materials.

MODELS DEVELOPMENT

FIB is a maskless patterning of material where the incident ions bombard on the substrate and removes substrate material atom by atom through cascades of collisions. Lenses, limiting apertures, and other electrostatic mechanisms are used to concentrate and guide the incident ions as a beam where the intensity distribution is assumed Gaussian. A deflection assembly is used to deflect the beam from pixel to pixel. The type of ion, acceleration voltage, intensity distribution, tailing and neighboring effects, and other beam parameters are analyzed in a group and described as beam function $\boldsymbol{B}$ for the development of models. The material properties, related to ion sputtering, are combined in a separate group called material function $\boldsymbol{M}$. These two functions are then combined to form the surface roughness function $\boldsymbol{R}$ as expressed by equation (1). The operator (*) represents any appropriate functional relationship.

$$[\boldsymbol{R}]=[\boldsymbol{M}]*[\boldsymbol{B}] \quad (1)$$

Beam Function

Beam function is developed for a 50 keV Ga ion FIB. The beam parameters include ion flux, beam profile, dwell time, limiting aperture, etc. Although the usual practice for the estimation of beam radius is to truncate the Gaussian beam where the beam intensity falls to a half (HWHM, 50%) or e^{-1} (37%) from its maximum level [Sato, 1997], they may not be valid when accurate surface roughness is required. So, in this analysis, the beam is truncated at a level where the intensity has fallen to e^{-f}. The value of f is different for different applications and determined by experiment. The following assumptions are made for the simplicity of analysis:

1. The beam cross section is circular (Fig. 1a).
2. The distance between two adjacent pixels (pixel distance) is constant.
3. The amount of redeposition is small and negligible.

Email: * mmyali@ntu.edu.sg

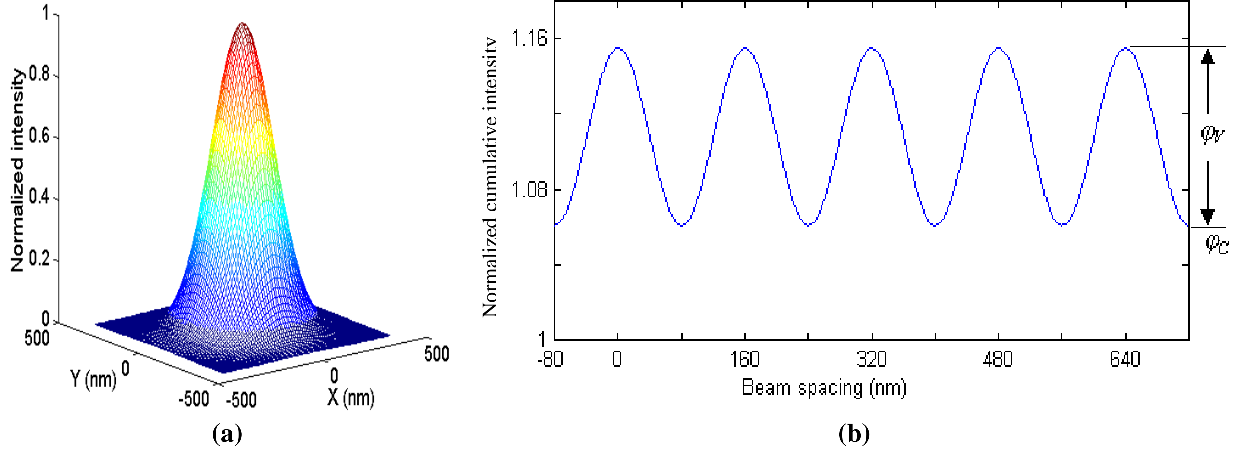

Fig. 1: (a) Normalized Gaussian intensity distribution of a FIB, (b) Cumulative intensity distribution.

4. The intensity distribution is Gaussian in two dimensions (Fig. 1a) and can be described by [Sato, 1997]:

$$\frac{J(x,y)}{J_0} = e^{\frac{-f(x^2+y^2)}{r^2}} \quad (2)$$

where,

$J(x,y)$ = beam intensity distribution at point x,y,
J_0 = peak intensity at the beam center,
x, y = coordinate of any point on the beam profile,
r = effective beam radius, and
f = a variable where e^{-f} represents a fraction of beam intensity insignificant to surface roughness.

When the beam scans, the cumulative intensity distribution becomes a periodic function which composed of a variable part (φ_V) and a constant part (φ_C) as shown in Fig. 1b. The function φ_V affects the surface finish while the function φ_C changes the base line of the surface profile. The analysis of periodicity and amplitude (a) shows that the function φ_V can be approximated as:

$$\varphi_V = a\cos^2\left(\frac{n}{2}+\frac{x}{D}\right)\pi \quad (3)$$

As the amplitude (a) was normalized with respect to flux (ϕ) and dwell time (T_C), the beam function can be written as:

$$\boldsymbol{B} = a\phi T_C \cos^2\left(\frac{n}{2}+\frac{x}{D}\right)\pi \quad (4)$$

Material Function

The material function represents the material behavior under the energetic FIB. In this subsection, this function is determined as an individual function to represent the response of material due to the interaction between the incident ions and the substrate atoms. Crystallographic directions and structures, atomic mass, binding energy, surface tension, sputtering yield, etc. are included in this function. The basic form of this material function is:

$$[\boldsymbol{M}] = [\boldsymbol{K_1}]*[\boldsymbol{K_2}] \quad (5)$$

where,

$\boldsymbol{M}$ = material function,
$\boldsymbol{K_1}$ = contribution due to crystallography to ion-atom interaction, and
$\boldsymbol{K_2}$ = contribution due to atomic properties of substrate to ion-atom interaction.

In this analysis, the factor $\boldsymbol{K_1}$ is normalized with respect to specific substrate material single crystal (100) silicon, i.e., $\boldsymbol{K_1} = 1$. Secondly, the factor $\boldsymbol{K_2}$ is determined by Sigmund's sputtering yield [Sigmund, 1981] divided by the substrate atomic density (η) to get the material removal in m^3/ion. So:

$$\mathbf{K_2} = \frac{Y(E)}{\eta} \quad (6)$$

Surface Roughness

A surface profile, formed by one raster of the ion beam sputtering, is considered for the development of surface roughness models. The following assumptions are made:

1. Beam radius (r) is bigger than the half of the pixel spacing (D). (i.e., $r > D/2$).
2. The ion flux and dwell time are sufficient to replicate the cumulative beam profile on the substrate by one raster (leaving no island between two beam centers).
3. The sputtered atoms are completely removed form the substrate leaving no redeposition.

The beam function just replicates its own functional shape if the material is "passive" that means the material function is unity. If the material function is not unity, then the surface profile of the sputtered feature is either a damped or a modified form of the beam function. The degree of such damping or modification depends on the material function. Higher value of beam function indicates longer and more energetic collisions, while a higher value of material function indicates that the material allows the beam to sputter more. So, the operator (*) between the beam function and material function in equation (1) is a multiplication. As the sputtered profile will be the inverse of the intensity profile, equation (1) can be rewritten by shifting the phase $\pi/2$ radians as:

$$\boldsymbol{R} = \boldsymbol{K_1 K_2}\, a\phi T_C \cos^2\left(\frac{n+1}{2} + \frac{x}{D}\right)\pi \tag{7}$$

Once the surface profile is available, surface roughness can be calculated from the established procedure [Whitehouse, 1994].

$$\boldsymbol{R_a} = \frac{\boldsymbol{K_1 K_2}\, a\,\phi\, T_C}{\pi} \tag{8}$$

$$\boldsymbol{R_t} = \boldsymbol{K_1 K_2}\, a\,\phi\, T_C = \pi\,\boldsymbol{R_a} \tag{9}$$

MODELS VERIFICATION

Surface Roughness Measurement

A 50 keV dual focused e $^-$/Ga ion beam (Micrion 9500EX) integrated with an energy dispersive X-ray (EDX) system (Oxford Link ISIS300) was used to sputter microsurfaces on a single crystal (100) silicon wafer. The 20 μm × 20 μm sized windows were sputtered by unidirectional beam scanning at factorial combination of beam parameters. The parameters were pixel spacing, ion dose, dwell time, and aperture size as listed in Table 1. Each of the experiments was replicated twice. The surface roughness at the bottom of the sputtered features were then measured using atomic force microscope (AFM) which included the measurement uncertainties of ±0.5 nm and ±1.0 nm for R_a and R_t respectively (Table 1). Since the line surface roughness was theoretically less than or equal to the area surface roughness, the measured area surface roughness was used conservatively for verification. Fig. 2 shows a typical sputtered bottom surface. The measured surface roughness values, along with theoretical values, are presented in Fig. 5.

Theoretical Surface Roughness

To calculate the theoretical surface roughness, the beam function and material function were determined first. After that, surface roughness was calculated by using models expressed by equations (8) and (9).

Experiments were performed on single crystal (100) silicon substrate to characterize the beam profile. FIB at factorial combination of beam parameters was directed to the four corners of 500 nm × 500 nm sized windows. The beam parameters were ion dose, dwell time, and aperture size. At these four points the ion beam replicated its own shape by sputtering four different craters with no significant interference of neighboring beams as shown in Fig. 3. An AFM (Dimensions 3000, Digital Instruments) was used for measuring the beam profile. The beam profiles were found well fitted with Gaussian curve to about three times of the standard deviations.

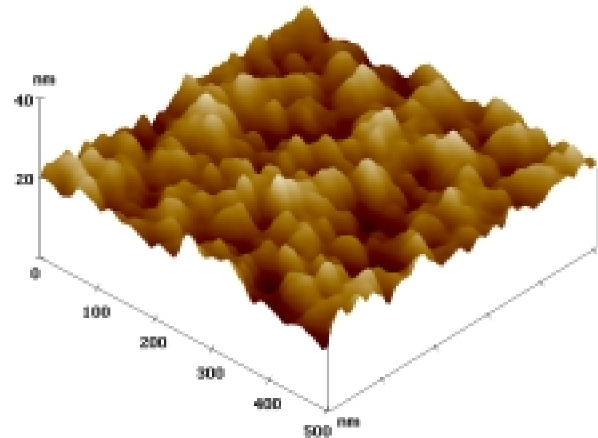

Fig. 2: AFM micrograph of FIB sputtered bottom surface profile on single crystal (100) silicon. Sputtering parameters: 50 keV Ga ion FIB, 150 μm aperture, 1 nC/μm^2 ion dose, 100 nm pixel spacing, and 50 μs dwell time.

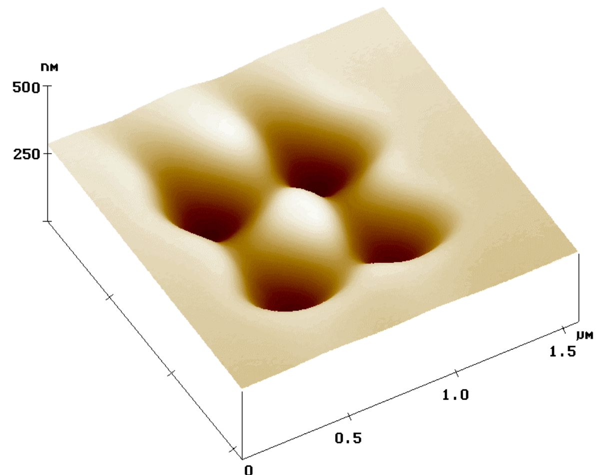

Fig. 3: AFM micrograph of FIB sputtered craters on single crystal (100) silicon. Sputtering parameters: 50 keV Ga ion FIB, 0.25 nC/μm^2 ion dose, 150 μm aperture, 500 nm pixel spacing, and 25 μs dwell time.

Table-1: Measured bottom surface roughness of FIB sputtered microfeatures on single crystal (100) silicon. (The measurement uncertainties are ±0.5 nm and ±1.0 nm for R_a and R_t respectively.)

Sample	Pixel spacing	Ion dose	Dwell time	Aperture size	Surface roughness (nm)	
#	nm	nC/μm^2	μs	μm	R_a	R_t
1a	25	1	25	150	1.5	8
1b	25	1	25	150	1.5	9
2a	100	1	25	150	2.0	11
2b	100	1	25	150	2.0	12
3a	25	3	25	150	2.0	10
3b	25	3	25	150	2.0	9
4a	100	3	25	150	2.5	12
4b	100	3	25	150	2.0	12
5a	25	1	50	150	1.0	8
5b	25	1	50	150	1.5	7
6a	100	1	50	150	2.0	10
6b	100	1	50	150	2.5	11
7a	25	3	50	150	1.5	7
7b	25	3	50	150	1.0	5
8a	100	3	50	150	2.0	12
8b	100	3	50	150	2.0	12
9a	25	1	25	300	1.0	5
9b	25	1	25	300	1.0	3
10a	100	1	25	300	1.0	7
10b	100	1	25	300	1.5	6
11a	25	3	25	300	1.0	2
11b	25	3	25	300	1.0	4
12a	100	3	25	300	1.0	7
12b	100	3	25	300	1.5	8
13a	25	1	50	300	1.0	7
13b	25	1	50	300	1.0	5
14a	100	1	50	300	2.0	8
14b	100	1	50	300	2.0	9
15a	25	3	50	300	1.0	4
15b	25	3	50	300	1.0	5
16a	100	3	50	300	2.0	9
16b	100	3	50	300	2.0	6

The average level of insignificant intensity was about 11% with a standard deviation of 1.5%. For bottom surface roughness models, the beam radius was then approximated as the half width where the intensity fell to $e^{-2.2}$ (11%) of the maximum level (i.e., f = 2.2).

Then the critical dwell time (T_C), the time to reach the steady state surface profile, is determined. This is the minimum time required to deliver the variable intensity of the cumulative profile. Beyond this time, the sputtered bottom surface profile remains the same but moves down gradually in every raster of sputtering. The critical dwell time was assumed inversely proportional to the peak normalized cumulative intensity I_{max} and directly proportional to the amplitude a as:

$$\frac{T_{C1}\, I_{1max}}{a_1} = \frac{T_{C2}\, I_{2max}}{a_2} \quad (10)$$

In the above equation, the subscripts "1" and "2" represent two different sputtering conditions where one of the T_C's is to be determined by experiment. The parameters a and I_{max} are to be known analytically from the cumulative intensity profile for any combination of beam radius and pixel spacing. For different sputtering conditions, the three parameters, ion flux, amplitude, and dwell time, were then combined to obtain the beam function $\boldsymbol{B}$.

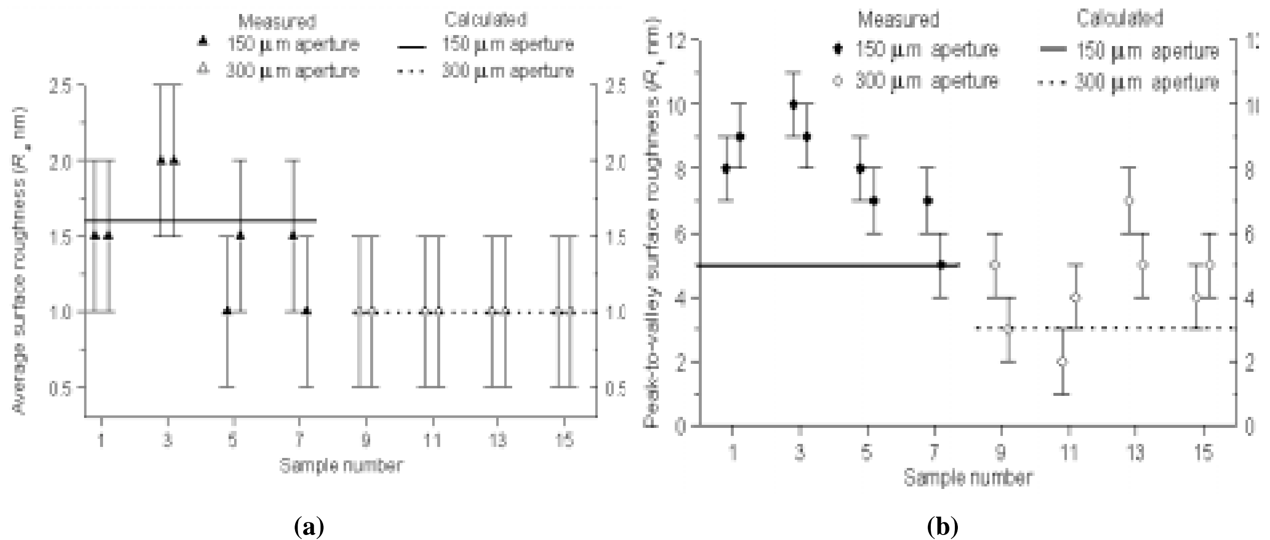

(a) **(b)**

Fig. 4: Comparison of measured and calculated bottom surface roughness values for the pixel spacing of 25 nm of the samples listed in Table 1. (a) Average surface roughness (R_a), (b) Peak-to-valley (maximum) surface roughness (R_t).

The analytical material function $\boldsymbol{M}$ reflects the interaction between the incident ions and the substrate atoms as expressed in equation (5). The sputtering yield was determined theoretically $Y(E)$ = 1.46 atoms/ion and then verified experimentally. For the silicon substrate, the factor $\boldsymbol{K_1}$ = 1. The factor $\boldsymbol{K_2} = 2.90\times10^{-29}$ m^3/ion for $Y(E)$ = 1.46 atoms/ ion, and atomic density $\eta = 5.08\times 10^{28}$ atoms/m^3.

Thus, when using Ga ion to sputter (100) silicon at the said parameters, the material function is reduced to:
$\boldsymbol{M} = 2.90\times10^{-29}$ m^3/ ion = 0.029 nm^3/ion.

Equations (8) and (9) were used directly to calculate the surface roughness using the values of the beam function and material function as discussed above. The comparison of measured and calculated surface roughness values is presented in Fig. 4. In this Fig., the measured surface roughness include the measurement uncertainties (σ_m) of ±0.5 nm and ±1.0 nm for the surface roughness of R_a and R_t respectively.

APPLICATIONS

The surface roughness models could be applied on any single crystal material to estimate the sputtered surface roughness. Various microcavities, e.g., rectangular blocks, microgears, microgear trains, etc. were produced on single crystal silicon and used for replication of polymer microcomponents. But as silicon was a brittle material, the cavity can not be used for many replication cycles. Then the surface roughness models were directly applied on nickel-beryllium alloy, a mold material, which could be used for mass replication cycles. Cavities of microgear and microgear train were produced on nickel-beryllium alloy and successfully used for the replication of plastic microcomponents for hundreds of molding cycles [Hung et al., 2001]. One of the cavities and replicated microcomponents are shown in Fig. 5. A bottom surface roughness of 30-50 nm and 300-400 nm for R_a and R_t respectively were observed on the microcavities and molded microcomponents.

CONCLUSIONS

Mathematical models for the calculation of surface roughness at the bottom of FIB sputtered microfeatures were developed, verified and applied successfully. This research showed:

1. The beam profile was found Gaussian. The beam diameter was the full width where the intensity reduced to $e^{-2.2}$ or 11% of the maximum intensity and varied mostly with beam current.
2. The combination of material and beam functions resulted the theoretical surface profile used for the development of surface roughness models.
3. The present models were developed specifically for 50 keV Ga ion FIB and (100) silicon. An extension of this model will consider other acceleration voltages and substrate materials with different crystallographic structure and orientation.
4. Both R_a and R_t were measured to characterize the surface quality at the bottom of FIB sputtered microfeatures. The same parameters were used for the generation of theoretical and experimental surface roughness to minimize ambiguity.

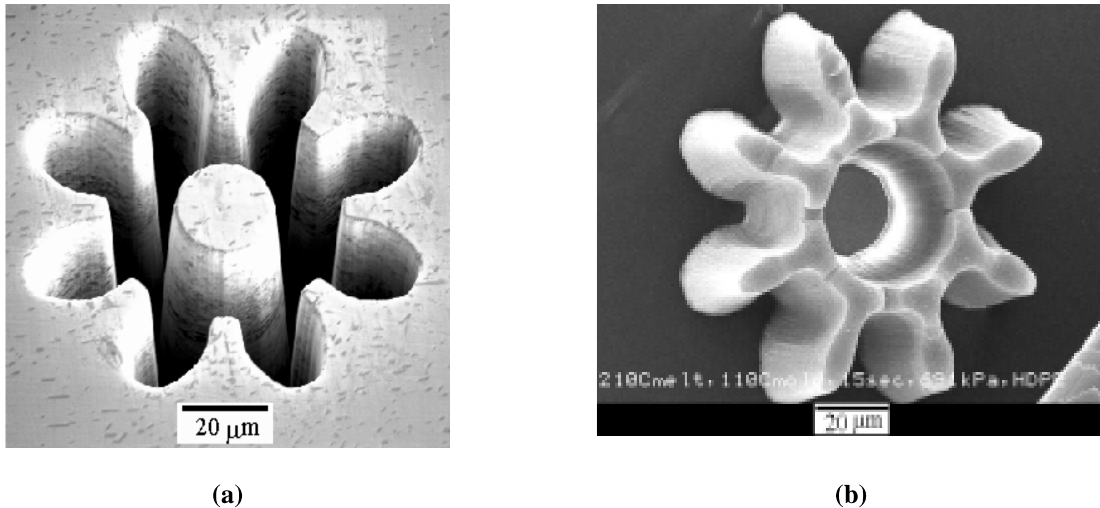

(a) **(b)**

Fig. 5: (a) Microgear cavity on nickel beryllium alloy. Sputtering parameters: 50 keV Ga ion FIB, 300 μm aperture, 300 nC/μm^2 ion dose, 36 nm pixel spacing, and 25 μs dwell time. (b) Molded microgear of HDPE. Molding parameters: 691 kPa injection pressure, 210° C melt temperature, 110° C mold temperature, and 15 s injection time.

5. The theoretical surface roughness was found to be within ±1 nm and ±5 nm of the measured surface roughness for R_a and R_t respectively.
6. The measured R_t was larger than the calculated R_t because of random deposition of sputtered atoms, fluctuations of beam current, and inconsistent arrival of incident ions.
7. Estimation of surface roughness within such few nanometers was of significant importance in the field of micromachining and microreplication processes.
8. For industrial applications, the required surface finish was 30-40 nm R_a for microoptical and micromechanical components [Weber et al., 1996] which could be achieved by FIB and LIGA.
9. Models were also directly applied on a mold material nickel beryllium alloy to fabricate microcavities and polymer microcomponents were replicated using these cavities.

ACKNOWLEDGMENTS

The authors would like to thank the Precision Engineering & Nanotechnology Center at Nanyang Technological University, Singapore, for its support.

REFERENCES

Ali, M.Y., Hung, N. P., and Yuan, S. "Simulation of Micro-Injection Molding", Int. Conf. on Precision Engineering, Singapore, 535-540 (2000).

Casey, J. D., Doyle, A. F., Lee, R.G., and Stewart, D.K. "Gas Assisted Etching with Focused Ion Beam Technology", *Microelectronic Eng.,* **24**, 43-50 (1994).

Ehrfeld, W., and Lehr, H. "Deep X-ray Lithography for the Production of Three-dimensional Microstructures from Metals, Polymers and Ceramics", *Radiation Physics and Chemistry,* **45** (3), 349-365 (1995).

Hung, N. P., Yuan, S., and Ali, M.Y "Development of Micromolding Process", **SPIE 4408**, 317-328 (2001).

Lorenz, H., Despont, M., Vettiger, P., and Renaud, P. "Fabrication of Photoplastic High-Aspect Ratio Microparts and Micromolds using SU-8 UV Resist", *Microsystem Tech.*, **4**, 143-146 (1997).

Ruprecht, R., Bacher, W., Haubelt, J.H., and Poitter, V. "Injection Molding of LIGA and LIGA-Similar Micro-structures using Filled and Unfilled Thermoplastics", **SPIE 2639**, 146-157 (1995).

Sato, M. "Resolution", *Handbook of Charged Particles Optics*, Orloff, J. (Ed.), CRC Press, NY, 319-361 (1997)

Sigmund, P. "Sputtering by Particle Bombardment: Theoretical Concept" *Sputtering by Particle Bombardment I*, Behrisch, R. (Ed.), Springer-Verlag, NY, USA, 9-25 (1981).

Vasile, M. J., Nasar, R., Xie, J., and Guo, H. "Microfabrication Techniques using Focused Ion Beams and Emergent Applications", *Micron-The Int. Research and Review J. for Microscopy*, **30 (3)**, 235-244 (1999).

Weber, L., Ehrfeld, W., Ferimuth, H., Lacher, M., Lehr, H., and Pech, B. "Micro Molding- A Powerful Tool for the Large Scale Production of Precise Microstructure", **SPIE 2879**, 156-167 (1996).

Whitehouse, D. J. "*Handbook of Surface Metrology*", IoP Publishing, Philadelphia, 5-90 (1994).